AGU PUBLICATIONS

JGR

Journal of Geophysical Research: Oceans

RESEARCH ARTICLE

10.1002/2014JC010462

Key Points:
- Taylor columns form above peaks in the South Scotia Ridge
- They markedly affect circulation and mixing in the Weddell-Scotia Confluence
- Conditions enable their formation elsewhere around the Scotia Sea and beyond

Correspondence to:
M. P. Meredith,
mmm@bas.ac.uk

Citation:
Meredith, M. P., A. S. Meijers, A. C. Naveira Garabato, P. J. Brown, H. J. Venables, E. P. Abrahamsen, L. Jullion, and M.-J. Messias (2015), Circulation, retention, and mixing of waters within the Weddell-Scotia Confluence, Southern Ocean: The role of stratified Taylor columns, *J. Geophys. Res. Oceans*, *120*, 547–562, doi:10.1002/2014JC010462.

Received 18 SEP 2014
Accepted 6 JAN 2015
Accepted article online 13 JAN 2015
Published online 29 JAN 2015

Circulation, retention, and mixing of waters within the Weddell-Scotia Confluence, Southern Ocean: The role of stratified Taylor columns

Michael P. Meredith[1], Andrew S. Meijers[1], Alberto C. Naveira Garabato[2], Peter J. Brown[1,3,4], Hugh J. Venables[1], E. Povl Abrahamsen[1], Loïc Jullion[2,5,6], and Marie-José Messias[3,7]

[1]British Antarctic Survey, Cambridge, UK, [2]University of Southampton, National Oceanography Centre, Southampton, UK, [3]School of Environmental Sciences, University of East Anglia, Norwich, UK, [4]Now at National Oceanography Centre, Southampton, UK, [5]Now at Aix-Marseille Université, CNRS/INSU, IRD, MIO, UM 110, Marseille, France, [6]Also at Université de Toulon, CNRS/INSU, IRD, MIO, UM 110, La Garde, France, [7]Now at University of Exeter, Exeter, UK

Abstract The waters of the Weddell-Scotia Confluence (WSC) lie above the rugged topography of the South Scotia Ridge in the Southern Ocean. Meridional exchanges across the WSC transfer water and tracers between the Antarctic Circumpolar Current (ACC) to the north and the subpolar Weddell Gyre to the south. Here, we examine the role of topographic interactions in mediating these exchanges, and in modifying the waters transferred. A case study is presented using data from a free-drifting, intermediate-depth float, which circulated anticyclonically over Discovery Bank on the South Scotia Ridge for close to 4 years. Dimensional analysis indicates that the local conditions are conducive to the formation of Taylor columns. Contemporaneous ship-derived transient tracer data enable estimation of the rate of isopycnal mixing associated with this column, with values of O(1000 m^2/s) obtained. Although necessarily coarse, this is of the same order as the rate of isopycnal mixing induced by transient mesoscale eddies within the ACC. A picture emerges of the Taylor column acting as a slow, steady blender, retaining the waters in the vicinity of the WSC for lengthy periods during which they can be subject to significant modification. A full regional float data set, bathymetric data, and a Southern Ocean state estimate are used to identify other potential sites for Taylor column formation. We find that they are likely to be sufficiently widespread to exert a significant influence on water mass modification and meridional fluxes across the southern edge of the ACC in this sector of the Southern Ocean.

1. Introduction

The Weddell-Scotia Confluence (WSC) lies above the complex bathymetry of the South Scotia Ridge in the Atlantic sector of the Southern Ocean (Figure 1). To the north of the WSC flows the Antarctic Circumpolar Current (ACC), the world's largest current system, which crosses the Scotia Sea and veers north having exited Drake Passage [*Meredith et al.*, 2011]. To the south of the WSC lies the cyclonic, subpolar Weddell Gyre, which is the site of significant dense water formation and throughflow [*Jullion et al.*, 2014]. Terminology has varied over time, but current nomenclature has it that the WSC is delimited to the south by the Weddell Front (WF), and to the north by the Southern Boundary of the ACC (Figure 1) [*Heywood et al.*, 2004; *Orsi et al.*, 1995].

Despite its location, it is clear that the waters of the WSC are not formed simply by mixing of the juxtaposed ACC and Weddell Gyre waters. Instead, they are characterized by significantly reduced stratification at intermediate depths compared with the waters on either side. Early concepts ascribed this to enhanced vertical mixing within the WSC itself [*Patterson and Sievers*, 1980], but subsequently it was noted that the injection of the shelf waters from close to the tip of the Antarctic Peninsula (Figure 1) into the WSC is likely to be more significant. These waters are characteristically cold and fresh, and, once injected, they can sink to intermediate depths and flow eastwards, mixing isopycnally to cool and freshen the WSC and beyond [*Whitworth et al.*, 1994].

Meridional transfers of water across the South Scotia Ridge and WSC are important in the regional and Atlantic-scale circulation, with dense Antarctic Bottom Water (AABW) being exported through deep gaps in

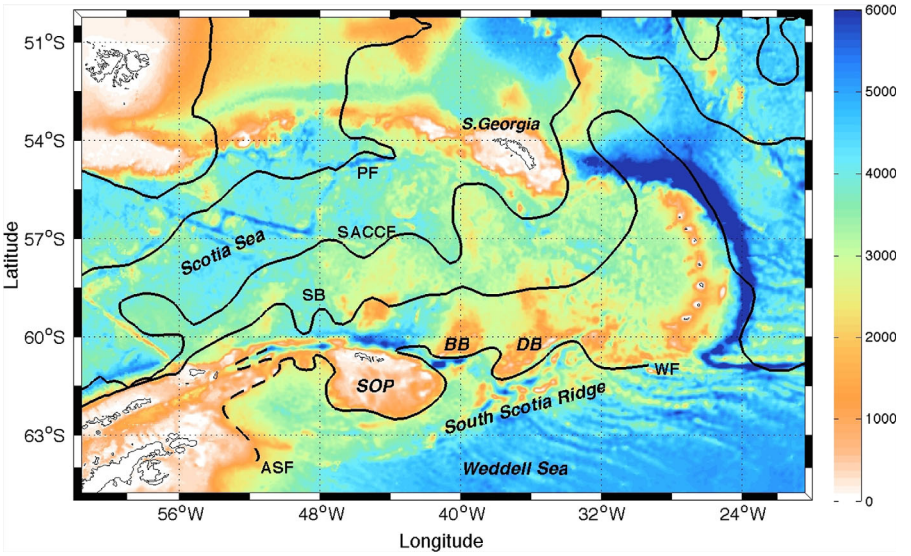

Figure 1. Topography of the Scotia Sea and surrounding environs. Selected topographic features along the South Scotia Ridge are marked, namely the South Orkney Plateau (SOP), Bruce Bank (BB), and Discovery Bank (DB). Various oceanographic fronts are marked, including the Polar Front (PF), the Southern ACC Front (SACCF), Southern Boundary of the ACC (SB), Weddell Front (WF), and Antarctic Slope Front (ASF; dashed). Frontal locations adapted from *Heywood et al.* [2004]; *Orsi et al.* [1995].

the ridge (most notably Orkney Passage, the deep passage between the South Orkney Plateau and Bruce Bank; Figure 1) [*Locarnini et al.*, 1993; *Naveira Garabato et al.*, 2002]. Opposing flows of AABW on opposite sides of the deep gaps that dissect the South Scotia Ridge have been noted using hydrographic and tracer data collected from sections conducted along its crest, with predominantly northward flows observed on the western sides of the clefts in the ridge, and southward flows on the eastern sides [*Naveira Garabato et al.*, 2002]. Having crossed the South Scotia Ridge and exited the Scotia Sea, AABW then flows northward replenishing the lower limb of the Atlantic meridional overturning circulation (AMOC), and it was suggested recently that a warming or reduction in the export of AABW can have a significant impact on the overall strength of the AMOC in the North Atlantic [*Patara and Böning*, 2014].

Simultaneously with the predominant northward export of AABW, intermediate-level exchanges also occur across the South Scotia Ridge [*Jullion et al.*, 2014]. From the north, the mid layer Circumpolar Deep Water (CDW) of the ACC can intrude southward towards the WSC. The lower component of CDW (LCDW), marked by a vertical salinity maximum in the ACC, is predominantly entrained into the Weddell Gyre at its eastern boundary (near 30°E; *Fahrbach et al.* [1994]). Within the Weddell Gyre, this water mass is greatly modified by mixing, becoming cooler and fresher at its core than the CDW to the north. It is typically termed Warm Deep Water (WDW) in the gyre, and penetrates the vicinity of the South Scotia Ridge from the south and west, having circulated cyclonically around the Weddell Sea.

In the upper levels, the surface circulation in the vicinity of the WSC is known to impact both local and remote ecosystem dynamics, with topographically steered currents (including that associated with the Antarctic Slope Front, ASF; Figure 1) transporting krill from their breeding/nursery grounds at the Antarctic Peninsula toward the Scotia Sea [*Hofmann et al.*, 1998; *Murphy et al.*, 2004]. In addition, the shelf waters of the Peninsula and surrounding island groups are known to have enhanced concentrations of micronutrients such as iron that are essential for promoting biological activity in the Southern Ocean, so their advection toward the southern Scotia Sea is believed to be a key factor in the enhancement of surface chlorophyll there [*Frants et al.*, 2012; *Thompson and Youngs*, 2013]. It has also been argued that eddies act to increase phytoplankton biomass in the WSC, and that eddy-mediated cross-frontal mixing of nutrients in this region has consequences for productivity in the southern part of the ACC [*Kahru et al.*, 2007].

Given the importance of circulation in the WSC and vicinity to both physical and ecological systems, it has been the focus of a number of recent studies, including the deployment of sets of drogued drifters [*Thompson et al.*, 2009; *Thompson and Youngs*, 2013]. These Lagrangian investigations have confirmed the strong

topographic steering of fronts such as the ASF and WF that was inferred previously from hydrographic section data [*Heywood et al*., 2004], but also revealed significant temporal variability in circulation and export associated with changing forcings.

The above studies have highlighted the need to understand the controls on circulation and variability in the region of complex topography spanned by the WSC. In practice, the South Scotia Ridge comprises a set of distinct but connected topographic obstructions of various scales and profiles (Figure 1). Elucidating the dynamics of the flow-topography interaction across these features is important to determining the influence of the ridge as a whole on the circulation and meridional transport of water masses.

The impacts that topographic obstacles can have on rotating flows have been the subject of significant attention since the early part of the twentieth century [e.g., *Proudman*, 1916; *Taylor*, 1923]. These early studies revealed that a stagnant cylinder of fluid can form above an obstacle in the path of a rotating flow, after which the circulation takes the form of a set of vertical columns of fluid that lie outside the stagnant region and which move without changing their length [*Taylor*, 1923]. The ''Taylor column'' is one possible outcome of a fluid flow impinging on an isolated topographic feature. As precursors to its formation, anticyclonic and cyclonic vortices can form as a consequence of the water column being compressed on the upstream flank of an obstacle to the flow, and stretched on the downstream flank. These vortices then rotate about the obstacle, but in certain flow conditions the cyclonic vortex will be discharged downstream and the anticyclonic vortex will adhere to the top of the mound.

Subsequent to their early recognition, the concept of Taylor columns has proved relevant across a range of disciplines, including their potential explanation for the Great Red Spot on Jupiter [*Hide*, 1961]. This wide relevance prompted considerable further research into their dynamics; for example Huppert [1975] conducted theoretical investigations into the initiation of steady Taylor columns in homogeneous and stratified fluids, while *Chapman and Haidvogel* [1992] used a primitive equation numerical model to investigate the conditions conducive to Taylor column formation.

The relevance of Taylor columns to oceanographic flows in the presence of topographic obstacles has been established in various locations, as has their impact on the functioning of the local biological systems [*Dower et al*., 1992; *Gould et al*., 1981; *Owens and Hogg*, 1980]. With reference to the Southern Ocean, *McCartney* [1976] studied theoretically the interaction of an eastward baroclinic current with a seamount, and found that the topographic obstacle led to the creation of a warm-core anticyclonic eddy above it.

A well-known example of a Taylor column in the Southern Ocean is the circulation above Maud Rise in the Weddell Sea [*Bersch et al*., 1992], which is believed to be significant due to its impact on vertical heat fluxes and hence polynya formation [*Muench et al*., 2001]. *Perissinotto and Duncombe-Rae* [1990] investigated the occurrence of mesoscale eddies at a topographic plateau south of Africa, and noted several similarities with theoretical predictions of Taylor column formation and structures, with strong biological impacts of the circulations also observed. *Meredith et al*. [2003] used data from Lagrangian drifters, ship-based surveys and satellites to demonstrate the presence of a strong but intermittent anticyclonic circulation above the Northwest Georgia Rise, an approximately 2000 m tall seamount immediately north of South Georgia (Figure 1). Remotely sensed ocean color data indicated that this circulation was marked by very high levels of chlorophyll, again reflecting the strong biological impact that these columns can have.

In this paper, we assess the potential role of Taylor columns in influencing the circulation, exchanges, and mixing in the vicinity of the WSC. A case study focusing on Discovery Bank on the South Scotia Ridge (Figure 1) is presented, using data from an intermediate-level Lagrangian float and a hydrographic/tracer section to quantitatively investigate the relevance of Taylor column dynamics, and the impact that the circulation has on water mass retention and transformation. The potential relevance of the findings beyond the locality of Discovery Bank is investigated using collected float and topographic data, and the output of an eddy-permitting Southern Ocean model constrained by observations.

2. Methods

2.1. Hydrographic and Tracer Data

Hydrographic data were obtained during the occupation of a transect along the crest of the South Scotia Ridge in March/April 2010, undertaken from the RRS *James Clark Ross* as part of the Antarctic Deep Water

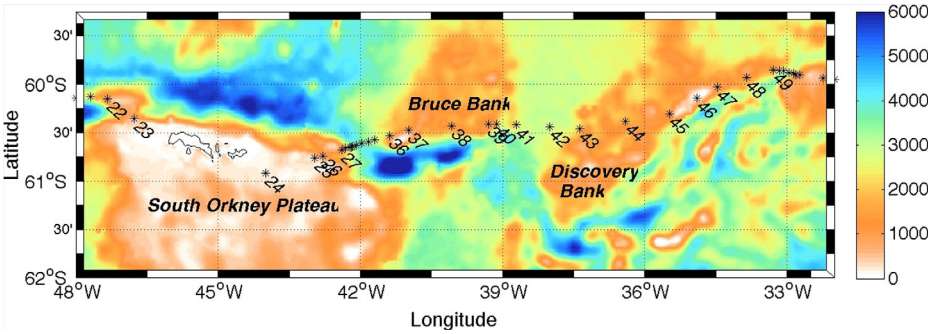

Figure 2. Locations of CTD/tracer stations used herein. Stations were conducted from RRS *James Clark Ross* during March 2010, as part of the Antarctic Deep Water Rates of Export (ANDREX) cruise.

Rates of Export (ANDREX) project [*Jullion et al.*, 2014]. Full details of data collection are given in *Meredith* [2010]; in brief, a SeaBird Electronics (SBE) 911+ Conductivity-Temperature-Depth (CTD) instrument mounted on a 24 position Niskin bottle frame was used to profile the full depth of the ocean to within 10 m of the seabed, with CTD conductivities calibrated using discrete bottle samples measured on a Guildline Autosal 9400B salinometer, and CTD temperatures calibrated using an SBE35 high-precision reference thermometer. Station locations relevant to this study are shown in Figure 2. Transient tracer data from the cruise are also used, specifically concentrations of dichlorodifluoromethane (CFC-12), trichlorofluoromethane (CFC-11), and sulphur hexafluoride (SF_6). Tracer concentrations were measured using a double purge-and-trap extraction technique, allied to two gas chromatographs with electron capture detectors. This combines the methods of *Smethie et al.* [2000] and *Law et al.* [1994], with a common valve for sample introduction. Water was drawn from the Niskin bottles, and concentrations calculated on the SIO-1998 scale relative to an external gaseous standard supplied by the National Oceanic and Atmospheric Administration (NOAA). Blank corrections were applied and duplicate analyses undertaken to determine analytical precision; these were found to be 1.4% or 0.005 fmol/kg (whichever is greater) for SF_6, 0.7% or 0.006 pmol/kg for CFC-12, and 0.5% or 0.009 pmol/kg for CFC-11.

2.2. Underway Velocity Data

During the ANDREX cruise, underway upper ocean velocity data were collected with a vessel-mounted Acoustic Doppler Current Profiler (ADCP). The instrument used was a 75 kHz RD Instruments Ocean Surveyor (OS75), operated predominantly in narrowband mode, and using bottom tracking when water depths were sufficiently shallow to permit (around 1100 m). The ADCP on RRS *James Clark Ross* is mounted in a transducer well containing 90% deionized water and 10% monopropylene glycol. The transducer depth is 6.3m, bin size was set to 16 m for narrowband mode, with a maximum bin depth of 1000 m. Position and attitude data are fed to the ADCP from a Kongsberg Seapath 200 GPS/inertial navigation instrument, and used to correct for ship's motion and attitude. Bottom track data were used to correct the ADCP velocity data for scaling and misalignment errors. When in bottom-track mode, data below 86% of the detected bottom depth were blanked. Automated and manual quality control was applied to remove outliers and sequences of obviously erroneous data. Tidal velocities were subtracted using the AntPen04.01 model, a high-resolution barotropic tidal model (1/30° × 1/60°, approximately 2 km) covering the domain 76°–58°S, 120°–30°W [*Padman et al.*, 2002].

2.3. Float Data

During the ANDREX cruise, an Argo float (ID 4501) was deployed at 09:45 UCT on 3 April 2010 at 60° 47.7'S, 39° 51.7'W, immediately south of Bruce Bank on the South Scotia Ridge. This was an ice-capable Argo float programmed to drift at 1000 m depth, sinking to 2000 m and rising to the surface at weekly intervals, and relaying the profiles of temperature, salinity, and pressure collected via satellite. The ice capability of the float ensured that it aborted its vertical ascents at times/locations where the hydrographic profiles indicated that risk of ice damage was determined to be significant. This led to significant gaps in the positional and profile data during the winter months, but ensured its longevity in an otherwise hostile environment. Standard automated Argo quality control led to the rejection of a large number of profiles from float 4501; however, manual quality control enabled many of the lost profiles to be retained in a finalized, cleaned data set.

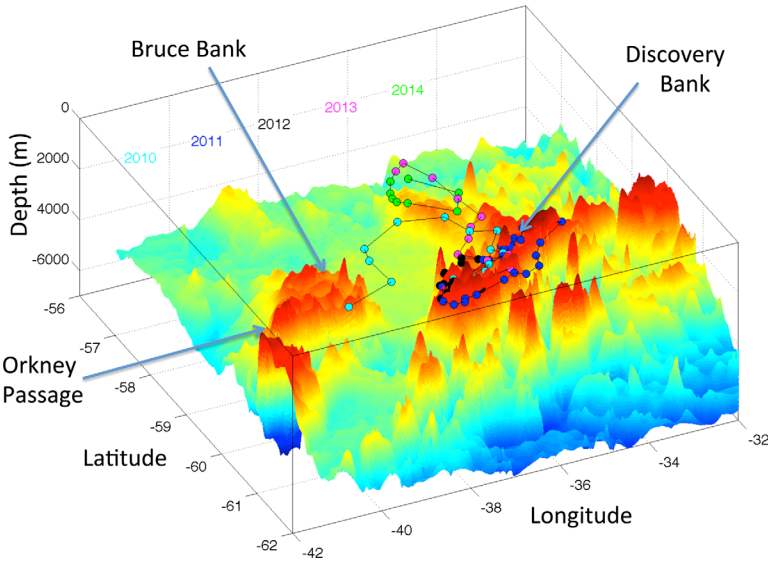

Figure 3. Trajectory of Argo float 4501 during 2010–2014. Float locations are color-coded by year: 2010 (cyan), 2011 (blue), 2012 (black), 2013 (magenta), and 2014 (green). The underlying topography is shown, with specific topographic features marked.

For regional scale analysis (section 3.4), all Argo paths that transited through the South Atlantic in the region 70°S–45°S and 70°–20° W in the period between January 2000 and June 2014 were examined. Only those paths with at least 10 data points in this region were included and only those that had the standard Argo delayed mode "good" quality control flag were used. This resulted in 342 float paths for analysis.

2.4. Regional Bathymetry and Model Fields

To examine the potential for Taylor column formation over the wider Scotia Sea area and beyond, regional metrics were calculated from bathymetric data and an assimilating Southern Ocean model. The bathymetric data were obtained from the General Bathymetric Chart of the Oceans (GEBCO) '08 1 min resolution grid, while 2008–2010 velocity and stratification fields were obtained from the Southern Ocean State Estimate (SOSE; full details in *Mazloff et al*. [2010]).

3. Results and Discussion

3.1. Circulation and Variability Above Discovery Bank

The trajectory of float 4501 for the 4 years after its deployment south of Bruce Bank is shown in Figure 3. The float initially moved eastward across the gap between Bruce Bank and Discovery Bank on the South Scotia Ridge (Figure 2), in accord with the predominantly eastward flows of the WSC. Upon encountering Discovery Bank in late 2010, the float commenced a series of closed circulations that relate strongly to the underlying topography (Figure 3); these persisted through to 2014. An initial closed loop over the southern part of Discovery Bank occupied most of 2011, after which a second closed loop occurred over this region in 2012 and early 2013. Following this, the float moved northward and completed a third closed loop (in late 2013 and 2014) over a deeper, northward extension of Discovery Bank in the Scotia Sea (Figure 3).

In practice, the trajectory shown in Figure 3 is derived from a subsampled set of positional data, since during periods of ice cover the float was unable to return either position or profile data. Consequently, while three closed loops in the vicinity of Discovery Bank are known to have occurred, there may have been yet more complexity to the circulation than is immediately apparent.

The float-derived profiles viewed in potential temperature-salinity space (Figure 4) provide insight into the location of the float relative to the local zonation of the waters as a function of time. They reveal that the float was deployed south of the WF (as indicated by the comparatively cool CDW, and the relatively high salinity of the temperature-minimum Winter Water (WW) layer). The float soon moved north of the WF as it traversed toward Discovery Bank, and thereafter spent most of the following 4 years in this oceanographic zone before moving north into the southern part of the ACC (comparatively high CDW potential

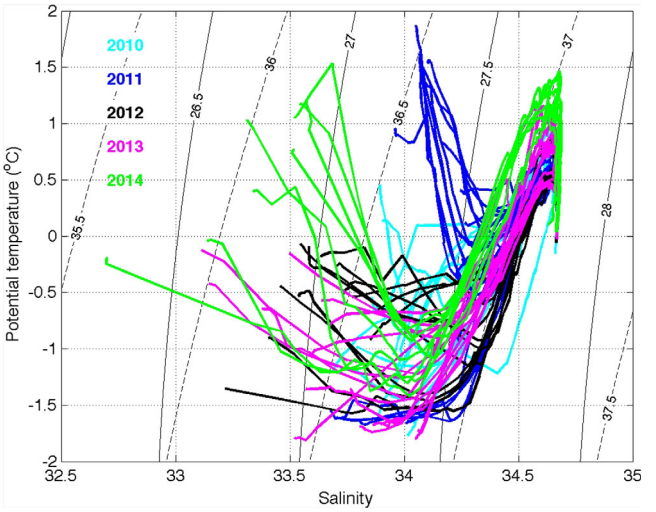

Figure 4. Potential temperature-salinity characteristics of the profile data recovered from Argo float 4501. Profiles are color-coded by year, as per Figure 3. Contours of constant density are marked (σ_0 solid; σ_2 dashed). Note the different profile in the temperature minimum WW layer and CDW layer in early 2010, before the float traversed north of the WSF.

temperature in 2014). There is considerable interannual variability in near-surface properties (Figure 4), reflecting not only the movement of the float through the oceanographic zonation but also the year-to-year changes in climatic forcing of the region. For example, the high near-surface temperatures observed in early 2011 are likely a response to the extremely strong La Niña event that occurred around then, and also a positive extreme of the Southern Annular Mode (SAM) that reached a record maximum in 2010 and persisted through into 2011. It is well established that both SAM and the El Niño/Southern Oscillation phenomenon have marked impacts on this sector of the Southern Ocean [*Ciasto and Thompson*, 2008; *Meredith et al.*, 2008; *Yuan*, 2004].

The remarkable 4 year residence time of Argo float 4501 above Discovery Bank, and the existence of at least three closed loops in its trajectory, suggest that Taylor column dynamics may play a significant role in dictating circulation here. The nature of the float's recirculations is complex, but this is not unexpected given the very contorted nature of the topography in this area. In essence, Discovery Bank is very different in shape and complexity to the cones/cylinders from which classical Taylor column dynamics were originally inferred, and hence one cannot expect rotational circulations to exist above it that are simple in structure or, given the potential time dependency of the circulation here, static.

3.2. The Role of Taylor Column Dynamics

To assess the potential relevance of Taylor column dynamics to the circulation above Discovery Bank more quantitatively, we here conduct a set of scaling analyses, as per *Huppert* [1975].

The Burger number, $B = NH/fL$, expresses the relative importance of local stratification to rotation, where N is the Brunt-Väisälä frequency, H is the depth beyond the topographic obstacle, f is the Coriolis parameter, and L is the horizontal length scale of the bathymetric feature. With $N \approx 10^{-3}$ s^{-1}, $H \approx 3000$ m, $f \approx 1.26 \times 10^{-4}$ s^{-1} and $L \approx 100$ km, one obtains $B \approx 0.25$.

The Rossby number, $R_o = U/fL$, compares the inertial and rotational terms of the equation of motion, where U is the horizontal velocity scale. Instantaneous velocities derived from the vessel-mounted ADCP (Figure 5) can be as high as 20 cm/s, whereas the long-term mean speed of Argo float 4501 is much lower (around 2–3 cm/s); this range gives an estimate of $R_o \approx 1 \times 10^{-3} - 1.5 \times 10^{-2}$. The scaled bump height is $h_o = h/H$, where h is the height of the topographic obstacle. For Discovery Bank, $h_o \approx 0.8$.

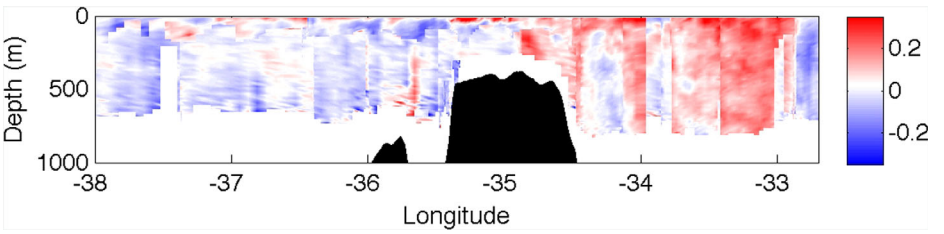

Figure 5. Meridional upper ocean velocities (m/s) from the vessel-mounted ADCP along the ship track marked in Figure 2. The peak of Discovery Bank is apparent.

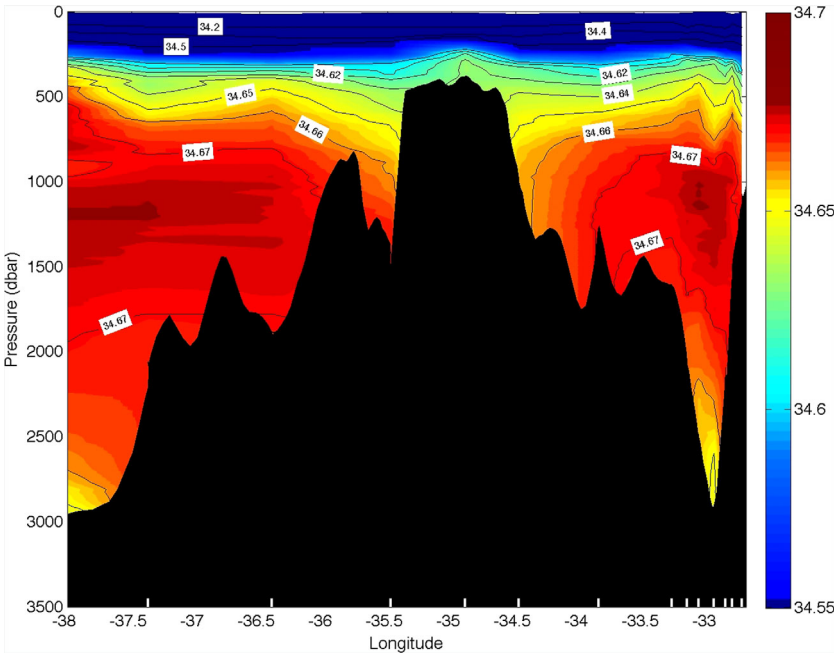

Figure 6. Salinity above Discovery Bank, from the ANDREX cruise in 2010. Station locations are marked by white ticks above the horizontal axis, and also shown in Figure 2.

Following *Huppert* [1975], for $B \approx 0.25$, the critical height for stratified Taylor column formation (expressed as h_o/R_o) is around 2–3. In the case of Discovery Bank and the circulation above it, h_o/R_o is 1–2 orders of magnitude greater than this, indicating that the circulation, stratification, and topography in this locality are indeed conducive to Taylor column formation.

It is noted that classical Taylor columns reside above the topographic obstacle that causes their formation, whereas the peak of Discovery Bank is shallower than the 1000 m level at which the Argo float drifts. However, there is good evidence that the circulation indicated by the float extends above the peak height of Discovery Bank to influence the waters up to the near-surface layers, and hence that the circulation is indeed a cromulent Taylor column. For example, the upper ocean velocities measured by the vessel-mounted ADCP during the ANDREX cruise (Figure 5) show predominantly northward velocities on the eastern side of Discovery Bank that extend throughout the full depth range ensonified (around 700–800m), while on the western side of Discovery Bank there are predominantly southward velocities.

Further evidence of the vertical extent of the column is obtained from the salinity and potential temperature fields from the ANDREX cruise (Figures 6 and 7 respectively). The isohalines are inclined downward toward the topography on both sides of Discovery Bank at depths between approximately 500–1500 m, consistent with the rotating flow observed in the float data. Above the peak of Discovery Bank itself, there is an upward doming of the isohalines. This is also apparent in the potential temperature section, where an upward doming of the isotherms is clear above the peak of Discovery Bank, consistent with the presence of a warm-core (anticyclonic) rotational feature that extends above the topography. The vertical extent of this doming extends into the WW layer, where a warm interruption above the peak of Discovery Bank is clear, with colder WW temperatures either side.

Whilst the conditions above Discovery Bank are conducive to Taylor column formation, and the circulation there has been seen to be consistent with this throughout much of the water column, it also appears that this circulation does not extend to the surface itself. For example, the vessel-mounted ADCP velocities (Figure 5) show northward flow at the surface on the eastern side of Discovery Bank, but on the western side the surface flow is less consistent in direction, and appears to show as many examples of northward flow as it does southward. Further, data from surface drifters (not shown), whilst sparse in this area, do not show any clear evidence of closed circulation features (S. Thorpe, personal communication, 2014). This is in

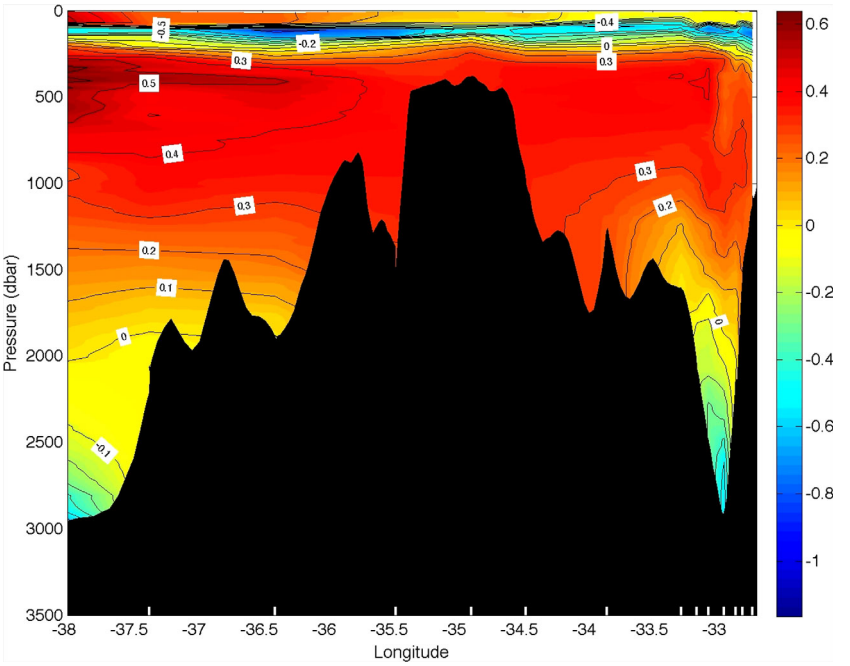

Figure 7. As for Figure 6, but for potential temperature (°C).

contrast to a number of other Taylor column features in the Southern Ocean, which have been observed to impact on the surface circulation and properties [*Bersch et al*., 1992; *Meredith et al*., 2003].

The absence of a clear surface signature of the Taylor column above Discovery Bank could be due to other processes dominating instead; for example, the presence of a surface Ekman layer and inertial currents could interrupt the column's structure and circulation. Alternatively, it is possible that the dynamical extent of the column falls short of influencing the surface itself: such columns are necessarily bottom intensified in stratified waters, and it is only when stratification permits that the column can reach the surface.

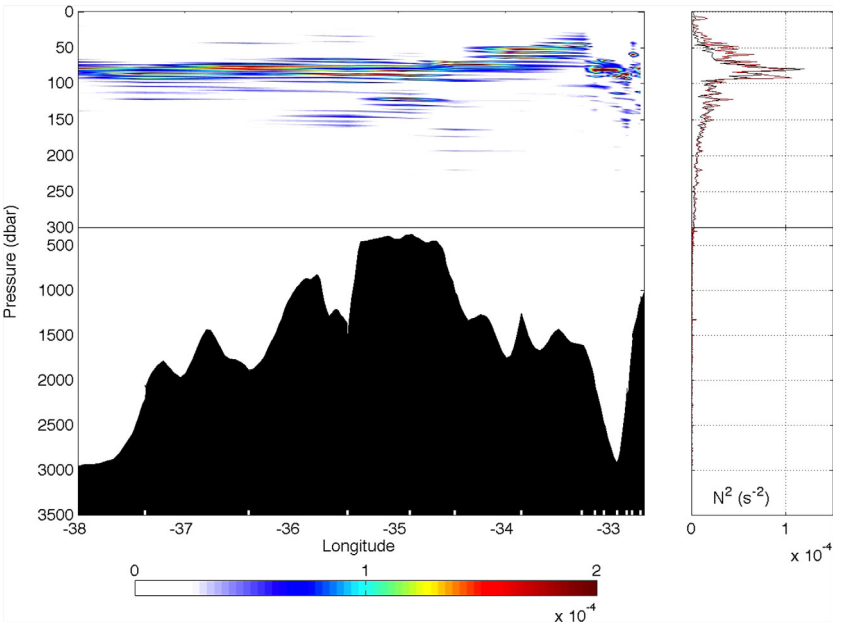

Figure 8. Left panel shows Brunt-Väisälä frequency squared (N^2) above Discovery Bank, from the ANDREX cruise in March/April 2010. Station locations are marked by white ticks above the horizontal axis, and also shown in Figure 2. The upper 300 dbar are shown on an expanded scale. The right plot shows the horizontal mean of N^2 (black line) and its standard deviation (red line).

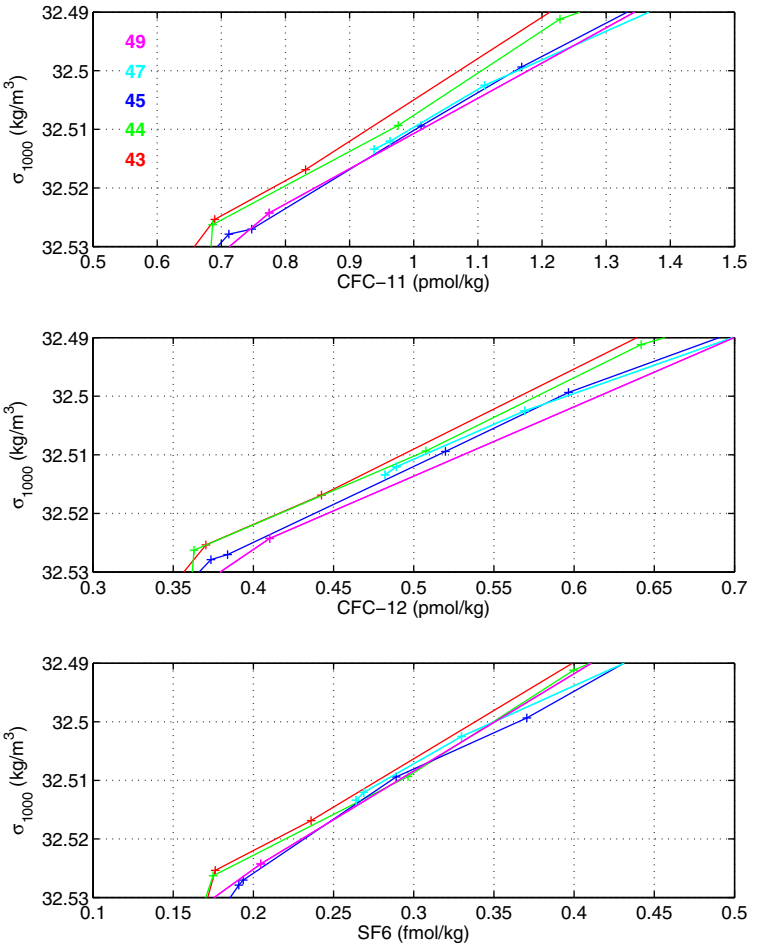

Figure 9. Profiles of (top) CFC-11 (middle) CFC-12, and (bottom) SF_6 versus potential density (referenced to 1000 m) obtained during the ANDREX cruise. Individual stations are color-coded, with station locations marked in Figure 2. For reference, the 1000 m level (the drift depth of Argo float 4501) is close to the $\sigma_1 = 32.525$ kg/m^3 surface.

To assess the likely vertical extent of the column, we calculate the decay height $H_d = fL/N$, which is the height above the seabed over which the effect of the column can be expected to be present [*Huppert*, 1975]. For the case of Discovery Bank, if $L \approx 100$ km and $N \approx 10^{-3}$ s^{-1}, one obtains $H_d \approx 13{,}000$ m. Under such circumstances, the column effect should be expected to reach the surface. However, the stratification above Discovery Bank (which is very weak in the deeper part of the water column) becomes relatively stronger in the near-surface pycnocline above approximately 200 m depth, with values for the Brunt-Väisälä frequency reaching approximately (1–3) $\times 10^{-2}$ s^{-1} (Figure 8). Under these circumstances, H_d is substantially reduced, becoming approximately 700–1300 m. It thus seems most likely that impact of the Taylor column on the circulation above Discovery Bank is substantially reduced in the surface layers due to the stronger stratification immediately below them, and that any effect that does penetrate to the surface is sufficiently small that it is overwhelmed by other processes that can influence the surface circulation directly.

3.3. Implications for Water Mass Transformation

The presence of a Taylor column above Discovery Bank, and its efficacy at retaining and stirring water in the local environment for multiyear periods, raise the possibility that such features may exert a significant influence on water mass modification in the area. To assess this quantitatively, we use transient tracer data collected during the ANDREX cruise, which include measurements on the western and eastern flanks of the column (Figure 2). The profiles of the transient tracers used are shown in Figure 9, adopting potential density rather than depth as the vertical coordinate due to the significant vertical excursions to which density surfaces are subjected as a consequence of the rotational circulation around the topographic obstacle (note the downward displacement of isohalines toward the topography in Figure 6).

The profiles of each of the transient tracer species considered fall into two distinct clusters (Figure 9). These are organized such that concentrations on the western side of Discovery Bank are slightly (but significantly) lower than those on the eastern side for densities at and above the $\sigma_1 \approx 32.525$ kg/m^3 surface. (This density surface is very close to the 1000 m level at which Argo float 4501 drifted when projected into depth space).

Given that the trajectory of Argo float 4501 indicated that a closed circulation exists over Discovery Bank, we interpret the difference in tracer concentrations across this feature as being indicative of relatively tracer-rich waters being fed into the column by entrainment on one flank, and relatively tracer-poor waters being fed into the column on the opposing flank. In essence, while the column itself will have closed streamlines associated with a rotating flow above the topography, isopycnal stirring will continuously exchange waters between the column and the ocean beyond its periphery. If the column sits in a field of tracer that has large-scale gradients in its vicinity, the stirring associated with the column's circulation will modulate the distribution of that tracer within the column itself. The tracer distribution observed is consistent with what is known about the tracer concentrations in the adjacent water masses here, which are higher in the CDW layers of the Scotia Sea and WSC than in waters of equivalent density further south in the Weddell Sea (see e.g., Figure 2 of *Meredith et al*. [2000]), as a consequence of the different mixing histories of these waters. While the large-scale tracer gradients are comparatively strong, mixing within the column will act to blend the waters isopycnally and reduce the tracer gradients relative to their initial concentrations. Given that water can reside within the column for multiyear periods and be subject to several rotations therein, the cumulative effect of the mixing has the potential to be significant, and hence can explain the more subtle differences in tracer concentrations on the opposing sides of the Taylor column.

It is noted that the tracer concentrations across Discovery Bank are lower on the western flank than the eastern. With the circulation around the bank being anticyclonic, this might be thought to run counter to the known large-scale tracer distribution in the region, which exhibits lower concentrations to the south. However, the locations at which water is injected into the circulation above Discovery Bank are influenced by the regional frontal locations, and in particular the convoluted path of the WF. This loops northward on the western side of Discovery Bank, and so will inject comparatively low-tracer waters north of the ANDREX cruise track on this side of the topography.

To estimate the rate of isopycnal mixing to which the waters entering the column are subject, we solve:-

$$K = V \frac{|C_W - C_e|}{|\frac{\partial C}{\partial y}|} \quad (1)$$

where K is an isopycnal diffusivity, V is the azimuthal velocity of the Taylor column, $Cw(e)$ is the tracer concentration on the western (eastern) flank, and $\partial C/\partial y$ is the large-scale meridional tracer gradient within which the Taylor column resides. This expression encapsulates the standard definition of the meridional eddy-induced (diffusive) transport of a tracer $(K|\frac{\partial C}{\partial y}|)$ as double the product of the eddy's azimuthal velocity (V), and the tracer anomaly it conveys ($C_w - (C_w + C_e)/2$).

To solve this, we use large-scale tracer gradients from a meridional section that crossed the South Scotia Ridge slightly downstream of Discovery Bank (at 31°W), and which extended from the northern Weddell Sea into the Scotia Sea. This was a repeat of a subset of the World Ocean Circulation Experiment section A23 [*Meredith et al*., 2013], and was conducted as part of the same ANDREX cruise in 2010 from which the data reported above were collected. (Using data collected on the same cruise avoids potential problems due to the temporal changes in tracer concentrations.) The equation is solved for the vertical level of Argo float 4501, with the mean azimuthal velocity obtained from the float trajectory (2–3 cm/s), and tracer concentrations from the profiles shown in Figure 9 ($C_w = 0.7$ pmol/kg, 0.37 pmol/kg, 0.17 fmol/kg for CFC-11, CFC-12, SF_6 respectively; $C_e = 0.75$ pmol/kg, 0.4 pmol/kg and 0.2 fmol/kg for CFC-11, CFC-12, SF_6 respectively).

Accordingly, we obtain isopycnal mixing rates in the Taylor column of 1000–1800 m^2/s. While this is necessarily a coarse estimate, the values are sufficiently large to be of significance to water mass transformation and modification. For example, these rates of isopycnal mixing are significant compared with those associated with transient mesoscale eddies in the southeast Pacific sector of the ACC (around 700 m^2/s; e.g., *Tulloch et al*. [2014]) and in Drake Passage [*Naveira Garabato et al*., 2011].

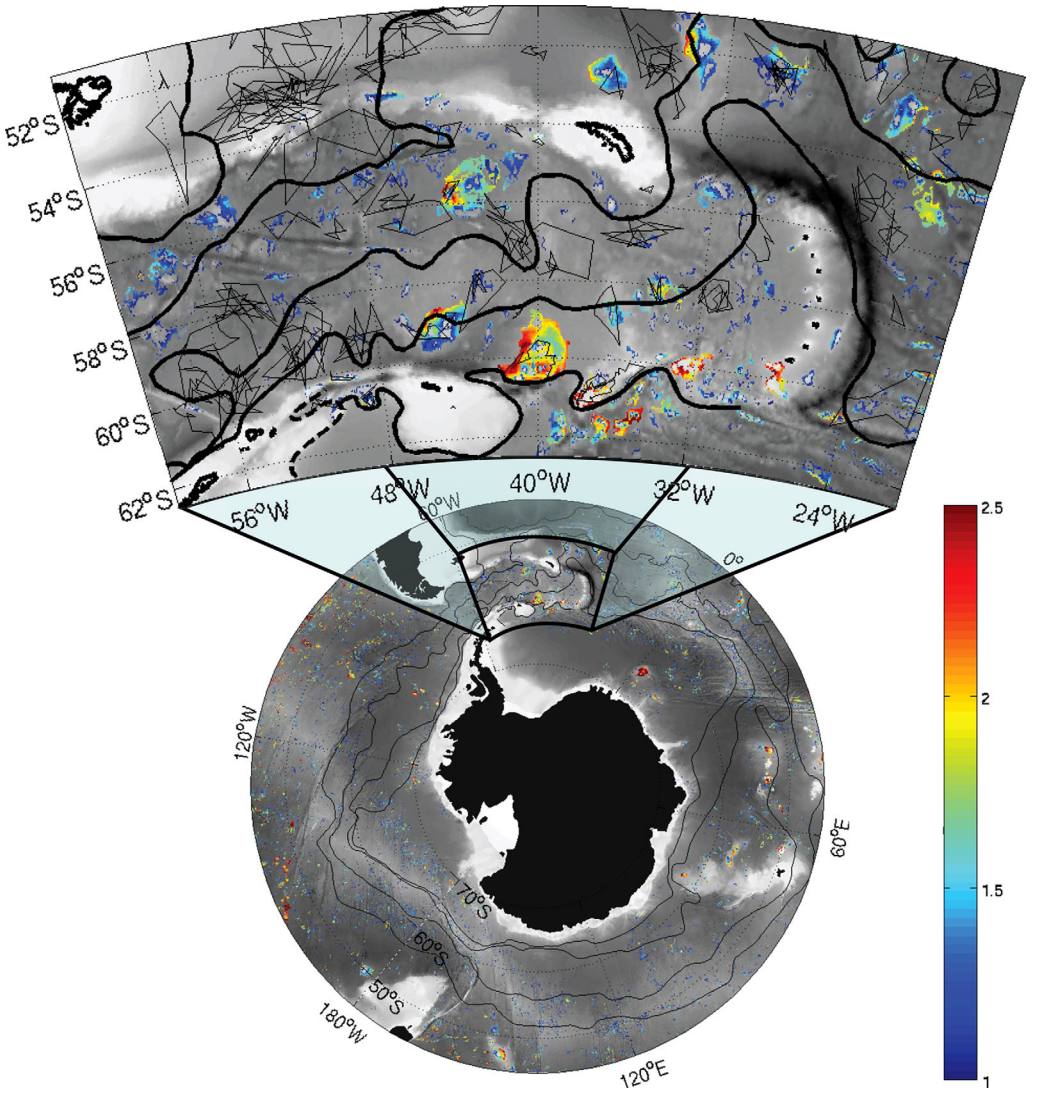

Figure 10. Regional and circumpolar maps of Taylor column distribution. Colored regions show the $\log_{10}$ of h_o/R_o over Taylor Column critical value, as calculated from regional bathymetry and SOSE model output using absolute velocities and stratification at 1000 m. Bold black lines show the approximate position of major Southern Ocean frontal features (as per Figure 1); fine black lines in the top plot show closed anticyclonic loops formed by Argo float trajectories.

3.4. Representativeness

To examine the representativeness of the above analysis, and to assess the extent to which Taylor column dynamics are relevant beyond the locality of Discovery Bank, we expand our analysis to include the broader Scotia Sea (Figure 10, top) and, for context, the circumpolar Southern Ocean (Figure 10, bottom). For this, we use the bathymetric data and SOSE model output detailed in section 2.4 to construct maps of a metric for the propensity for Taylor column formation, defined as the ratio between h_o/R_o divided by the critical value for Taylor column formation based on the Burger number B. Closed contours of bathymetric depth were calculated at 100 m depth intervals, and only those containing peaks (i.e., a mean depth shallower than the contour) were retained in the analysis. The scale of the peak relative to the depth of each contour around the peak (h_o) was calculated at each contour, thus for progressively shallower contours around a central peak the value will approach zero. This value will tend to underestimate the critical height for stratified Taylor column formation (h_o/R_o) toward the center of bathymetric features, and thus make our estimates conservative. R_o was calculated using U from the absolute SOSE velocity at 1000 m (the default Argo parking depth), while the horizontal length scale L was calculated as the radius of a circle centered on the mean latitude and longitude of each closed contour and sized such that the root mean square (RMS) difference between the points of the closed contour and fitted circle was minimized. This RMS value, normalized

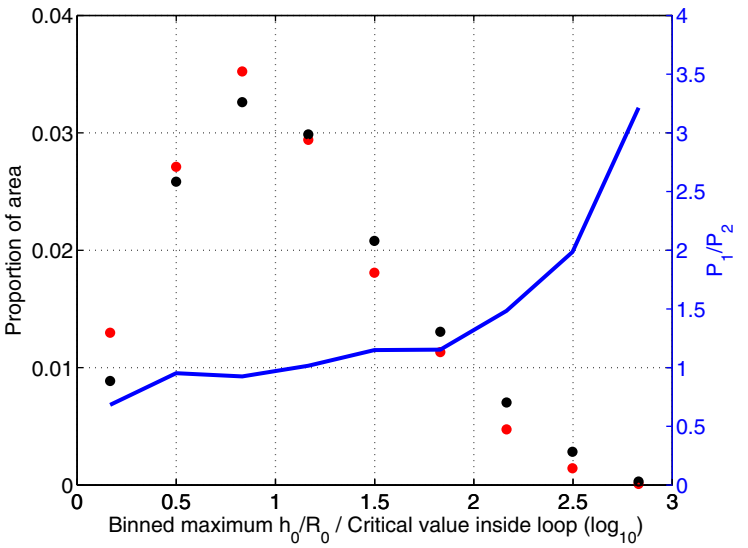

Figure 11. Proportion of the total area within the Scotia Sea occupied by ($\log_{10}$) values of h_o/R_o divided by the Taylor column critical height (P_2, red) binned in 0.33 increments, compared with the proportion of the total area enclosed within anticyclonic Argo loops occupied by values of h_o/R_o divided by the Taylor column critical height (P_1, black). The ratio between the two relative areas for each bin is given by P_1/P_2 (blue line).

by the radius of the circle, is also used to define the eccentricity of each closed contour; contours with an eccentricity greater than 0.005 were excluded from the analysis. This leads to some elongated features such as the northeast ridge of Discovery Bank being excluded, but the noisiness of the resulting R_o fields is significantly reduced and more closely depicts the actual conditions appropriate for Taylor column formation.

Figure 10 shows that regions of significant h_o/R_o are common over the southern part of the Scotia Sea and elsewhere, and particularly prevalent in the region of the WSC. For many of these features, including parts of Discovery Bank, h_o/R_o is 1–2 orders of magnitude greater than the critical value required for Taylor column formation. Also shown in Figure 10 (top) is the distribution of closed anticyclonic loops in the 342 Argo paths that pass through the Scotia Sea region. Only anticyclonic loops that consist of at least five points were considered, resulting in 262 individual loops. The majority of these loops appear in regions of significant mesoscale eddy energy, such as between the Subantarctic and Polar Fronts north of the North Scotia Ridge and in the Argentine Basin (not shown), in frontal meanders, or downstream of topography such as the Shackleton Fracture Zone. However, several looping Argo paths are also found over and around regions with large h_o/R_o relative to the critical value. This obviously includes the convoluted path around Discovery Bank discussed in section 3.1, but also examples around Bruce Bank, north and west of Orkney Plateau, and north and southwest of South Georgia. The feature immediately north of South Georgia is the Taylor column above the Northwest Georgia Rise, described previously by *Meredith et al.* [2003].

It is noted that Bruce Bank on the South Scotia Ridge is an especially clear example of a feature above which Taylor columns are likely to form, and indeed the available Argo data support this (Figure 10, top). The ANDREX section crossed this feature; however, the data from this are not used here for tracer-based mixing calculations because a pronounced transient eddy feature was resident in Orkney Passage at the time of the cruise, and distorted greatly the hydrographic and tracer fields on the western side of the bank.

Placing these results in a circumpolar context (Figure 10, bottom), it can be seen that the Scotia Sea is disproportionately important as a region of Taylor column formation along the path of the ACC, a consequence of its rugged bathymetry associated with the ridge systems and seamount chains that mark its periphery. Nonetheless, there are other regions within the ACC that show significant propensity toward Taylor column formation, most notably the region around the Kerguelen Plateau (near 70°E) and the bathymetric features that lie immediately upstream. Maud Rise in the Weddell Sea (close to the Greenwich Meridian) is easily identifiable as a feature of strong relevance to Taylor column dynamics.

Regions of topography with h_o/R_o exceeding zero comprise 14% of the total area of the Scotia Sea between 70°S–45°S and 70°W–20°W and deeper than 1000 m. Topography with h_o/R_o greater than zero also

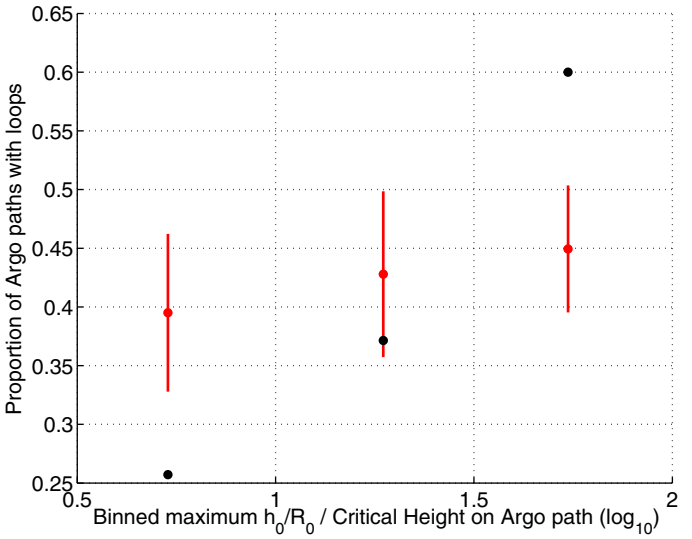

Figure 12. Proportion of Argo paths intersecting topography with a maximum value of h_o/R_o divided by the Taylor column critical height that also contain an anticyclonic loop (black dots), binned by maximum h_o/R_o divided by the Taylor column critical value ($\log_{10}$, increments of 0.5). Red dots (with two standard deviation error bars) give the proportion of loops predicted by the length of Argo paths within the bin (see text for details).

comprises 14% of the area enclosed within the 262 anticyclonic loops formed by Argo floats, suggesting that the presence of a topographic feature with raised h_o/R_o is not associated with an increased likelihood of an Argo float forming an anticyclonic loop around it. When the actual value of the enclosed h_o/R_o is taken into account however, this relationship changes (Figure 11). For values of h_o/R_o less than one order of magnitude greater than the critical value, the proportion of area with this value inside float loops is smaller than the proportion of the overall Scotia Sea with this value. This implies that closed Argo loops tend to be found away from these regions rather than over them. For values of h_o/R_o exceeding one order of magnitude greater than the critical value, this is reversed and closed Argo loops contain a greater fraction of these values relative to their frequency over the whole region. This relationship increases with greater h_o/R_o relative to the critical value, and values of h_o/R_o 300–1000 times the critical value occupy a fraction of area within Argo loops that is 2–3 times greater than the fraction of area occupied by these values over the whole region. This indicates that higher values of h_o/R_o relative to the critical value have an increased likelihood of closed Argo loops forming around them, and indicates significantly greater propensity for Taylor column formation above these features.

We also find that there is a clear relationship between the maximum h_o/R_o relative to the critical value encountered by a float along its trajectory and the likelihood of that float path having at least one anticyclonic loop (Figure 12). As the maximum value of h_o/R_o relative to the critical value encountered by a given float increases, so does the proportion of paths that include a loop. Care must be taken in interpreting this relationship, since the likelihood of an Argo path containing a closed loop and intersecting high h_o/R_o values both naturally depend strongly on the path length. However, when this factor is taken into account, we find that the Argo paths passing over a maximum value of h_o/R_o less than one order of magnitude greater than the critical value have a smaller proportion of loops (25% of paths) than would be predicted based on their path length alone (around 40%), or by the background rate at which loops occur in paths that do not encounter topography (37%; not shown). Those floats encountering values of h_o/R_o 30–100 times greater than the critical value have loops in 60% of cases, significantly more than would be predicted based on their path lengths (45%). As in Figure 11, a value of h_o/R_o approximately one order of magnitude greater than the critical value is the point at which loops appear around topography more frequently than the regional background rate. (The larger bin sizes used for h_o/R_o relative to the critical value in Figure 12 compared with Figure 11 are necessitated by the small sample size of float paths encountering h_o/R_o values. Here $n>10$ for each bin in each analysis.)

These analyses show that there is a clear relationship between closed loops in Argo paths and the presence of high h_o/R_o values relative to the critical number in the Scotia Sea. Although these relationships do not directly show causality between the topography and looping float paths, they strongly suggest that Argo floats preferentially form anticyclonic loops in the presence of topography with h_o/R_o at least one order of magnitude greater than the critical value, and that this tendency increases as the ratio of h_o/R_o to the critical value increases. Interestingly, both statistical analyses (Figures 11 and 12) suggest that loops form less frequently than the regional background rate in the presence of values of h_o/R_o less than one order of magnitude greater than the critical value. This may be due to these topographic features having a steering effect

that is strong enough to prevent the meanders and eddies that typically form closed loops away from topography, but not strong enough to drive the float in a complete closed loop around the feature. Such deflections due to weak Taylor columns or strong background flows will not be captured in the statistics presented here, and may mean that this analysis underrepresents the true prevalence of Taylor column dynamics in the region. Despite this, these statistical analyses and the qualitative distribution of closed loops in relation to h_o/R_o values in Figure 10 provide strong evidence that Taylor columns are relatively widespread in the Scotia Sea, and significantly modulate the regional circulation as it interacts with the complex bathymetry of the area.

4. Conclusions

The Scotia Sea is a key junction in the Southern Ocean circulation, with the waters of the ACC traversing it from west to northeast, while waters from the subpolar Weddell Gyre impinge on it from the south. Separating these contrasting flow regimes is the WSC, exchanges across which are important both physically and ecologically. We have demonstrated that the rugged topography that typifies the edges of the Scotia Sea, combined with the characteristic stratification and circulation of the regional flows, yield circumstances that are often conducive to the formation of stratified Taylor columns. The impact of these columns on the regional flows is notable: for example, the circulation above Discovery Bank on the South Scotia Ridge was seen to retain an intermediate-level float for close to 4 years, and to effect isopycnal mixing at a significant rate (order of 1000 m^2/s or more). A concept emerges of Taylor columns on the southern edge of the Scotia Sea being slow, steady blenders, and acting to retain the waters in the vicinity of the WSC for lengthy periods, during which they can be subject to significant modification.

There are numerous implications of these findings. The rate of isopycnal mixing derived here, while coarse and obtained from a single column feature, is significant compared with that effected by transient eddy features further north in the ACC, where mesoscale variability is typically much more intense. This suggests that the Taylor column features at the southern edge of the ACC may play a significant role in mediating isopycnal exchanges between the ACC's southern rim and the northern edge of the Weddell Gyre.

We have not diagnosed the rate of diapycnal mixing associated with the Taylor columns observed here. Nonetheless, we note that the retentive nature of these columns means that the water trapped within them will be exposed locally to such mixing for lengthy periods (up to several years). Diapycnal mixing in the Southern Ocean is typically elevated above complex topography, thus if the rate is indeed significant, this may act to locally increase the homogeneity of the water column. Such homogeneity is a key defining feature of the WSC, and while we do not assert that the Taylor column dynamics represent the leading-order mechanism in producing it, they may, however, contribute to the level of homogeneity observed.

Of the exchanges across the South Scotia Ridge, significant importance is attached to the export of dense AABW from the Weddell Sea. This is known to have warmed, freshened, and/or declined in flux in recent decades, with possible impacts on the lower limb of the overturning circulation along the length of the Atlantic. Opposing flows throughout the water column on the different sides of each of the gaps in the South Scotia Ridge have been reported previously. This is seen here to be consistent with the marked propensity for the topographic features separating the gaps to form Taylor columns, and suggests that these dynamics may have relevance for dense water export/recirculation processes in this key region of outflow.

In other areas, Taylor columns have been noted to have significant biogeochemical and biological implications. It is not our intention to explore these here directly, however, we note that the circulation above Discovery Bank did not extend completely to the surface, and hence would not necessarily have the same biological impact as a column that retained locally the waters of the euphotic zone for extensive periods. Nonetheless, the numerous other sites on the South Scotia Ridge that have been seen to be conducive to Taylor column formation indicate that other such features in the vicinity may have more significance biologically. This will be the focus of future studies.

When our regional analyses are extended circumpolarly, we find that the Scotia Sea is a marked hotspot for Taylor column formation within the Southern Ocean, and that other regions are typically much less significant in this context. This is consistent with the Scotia Sea having unusually complex topography and being fringed by chains of seamounts. Consequently, it may be disproportionately important in terms of

exchanging water and tracers across the southern edge of the ACC. It should be noted, however, that other selected regions appear significant (e.g., the area around and upstream of Kerguelen Plateau), and the processes identified here may be locally important in those regions also.

Acknowledgments
We thank the officers, crew, and scientific party of RRS *James Clark Ross* cruise JR235/6/9 (ANDREX) for assistance in acquiring the data used here. The ANDREX project was supported by the Natural Environment Research Council via award NE/E013368/1. ANDREX cruise data are available from the CLIVAR and Carbon Hydrographic Data Office (CCHDO; http://cchdo.ucsd.edu/). Southern Ocean Argo float data are available from the British Oceanographic Data Centre (BODC; http://www.bodc.ac.uk/projects/international/argo/southern_ocean/). Dr. Angelika Renner is thanked for work with the VM-ADCP data. Dr. Sally Thorpe is thanked for advice concerning surface drifters. We are grateful to Dr. Sebastiaan Swart and an anonymous reviewer for insightful comments that helped improve this paper. This paper is a contribution of the British Antarctic Survey (BAS) Polar Oceans programme.

References

Bersch, M., G. A. Becker, H. Frey, and K. P. Koltermann (1992), Topographic effects of the Maud Rise on the stratification and circulation of the Weddell Gyre, *Deep Sea Res., Part A*, *39*, 303–331.

Chapman, D. C., and Haidvogel (1992), Formation of Taylor caps over a tall isolated seamount in a stratified ocean, *Geophys. Astrophys. Fluid Dyn.*, *64*, 31–65.

Ciasto, L., and D. Thompson (2008), Observations of large-scale ocean–atmosphere interaction in the southern hemisphere, *J. Clim.*, *21*, 1244–1259.

Dower, J., H. Freeland, and K. Juniper (1992), A strong biological response to oceanic flow past Cobb Seamount, *Deep Sea Res., Part A*, *39*, 1139–1145.

Fahrbach, E., G. Rohardt, M. Schröder, and V. Strass (1994), Transport and structure of the Weddell Gyre, *Ann. Geophys.*, *12*, 840–855.

Frants, M., S. T. Gille, M. Hatta, W. T. Hiscock, M. Kahru, C. I. Measures, B. G. Mitchell, and M. Zhou (2012), Analysis of horizontal and vertical processes contributing to natural iron supply in the mixed layer in southern Drake Passage, *Deep Sea Res., Part II*, *90*, 68–76.

Gould, W. J., R. Hendry, and H. E. Huppert (1981), An abyssal topography experiment, *Deep Sea Res., Part A*, *28*, 409–440.

Heywood, K. J., A. C. Naveira Garabato, D. P. Stevens, and R. D. Muench (2004), On the fate of the Antarctic Slope Front and the origin of the Weddell Front, *J. Geophys. Res.*, *109*, C06021, doi:10.1029/2003JC002053.

Hide, R. (1961), Origin of Jupiter's great red spot, *Nature*, *190*, 895–896.

Hofmann, E. E., J. M. Klinck, R. A. Locarnini, B. A. Fach, and E. J. Murphy (1998), Krill transport in the Scotia Sea and environs, *Antarct. Sci.*, *10*, 406–415.

Huppert, H. E. (1975), Some remarks on the initiation of inertial Taylor columns, *J. Fluid Mech.*, *67*, 397–412.

Jullion, L., et al. (2014), The contribution of the Weddell Gyre to the lower limb of the Global Overturning Circulation, *J. Geophys. Res. Oceans*, *119*, 3357–3377, doi:10.1002/2013JC009725.

Kahru, M., B. G. Mitchell, S. T. Gille, C. D. Hewes, and O. Holm-Hansen (2007), Eddies enhance biological production in the Weddell-Scotia Confluence of the Southern Ocean, *Geophys. Res. Lett.*, *34*, L14603,doi:10.1029/2007GL030430.

Law, C. S., A. J. Watson, and M. I. Liddicoat (1994), Automated vacuum analysis of sulphur hexafluoride in seawater: Derivation of the atmospheric trend (1970–1993) and potential as a transient tracer, *Mar. Chem.*, *48*, 57–69.

Locarnini, R. A., T. Whitworth, and W. D. Nowlin (1993), The importance of the Scotia Sea on the outflow of Weddell Sea deep water, *J. Mar. Res.*, *51*, 135–153.

Mazloff, M. R., P. Heimbach, and C. Wunsch (2010), An eddy permitting Southern Ocean state estimate, *J. Phys. Oceanogr.*, *40*, 880–899.

McCartney, M. S. (1976), The interaction of zonal currents with topography with applications to the Southern Ocean, *Deep Sea Res. Oceanogr. Abstr.*, *23*, 413–427.

Meredith, M. P. (2010), Cruise Report, *RRS James Clark Ross, JR235/236/239*, p. 146., Brit. Antarct. Surv., Cambridge, U. K.

Meredith, M. P., R. A. Locarnini, K. A. Van Scoy, A. J. Watson, K. J. Heywood, and B. A. King (2000), On the sources of Weddell Gyre Antarctic bottom water, *J. Geophys. Res.*, *105*, 1093–1104.

Meredith, M. P., J. L. Watkins, E. J. Murphy, N. J. Cunningham, A. G. Wood, R. Korb, M. J. Whitehouse, S. E. Thorpe, and F. Vivier (2003), An anticyclonic circulation above the Northwest Georgia Rise, Southern Ocean, *Geophys. Res. Lett.*, *30*, 2061, doi:10.1029/2003GL018039.

Meredith, M. P., E. J. Murphy, E. J. Hawker, J. C. King, and M. I. Wallace (2008), On the interannual variability of ocean temperatures around South Georgia, Southern Ocean: Forcing by El Niño/Southern Oscillation and the Southern Annular Mode, *Deep Sea Res., Part II*, *55*, 2007–2022.

Meredith, M. P., et al. (2011), Sustained monitoring of the Southern Ocean at Drake Passage: Past achievements and future priorities, *Rev. Geophys.*, *49*, RG4005, doi:10.1029/2010RG000348.

Meredith, M. P., P. J. Brown, A. C. Naveira Garabato, L. Jullion, H. J. Venables, and M. J. Messias (2013), Dense bottom layers in the Scotia Sea, Southern Ocean: Creation, lifespan and destruction, *Geophys. Res. Lett.*, *40*, 933–936,doi:10.1002/grl.50260.

Muench, R. D., J. H. Morison, L. Padman, D. Martinson, P. Schlosser, B. Huber, and R. Hohmann (2001), Maud Rise revisited, *J. Geophys. Res.*, *106*, 2423–2440.

Murphy, E. J., S. E. Thorpe, J. L. Watkins, and R. Hewitt (2004), Modeling the krill transport pathways in the Scotia Sea: Spatial and environmental connections generating the seasonal distribution of krill, *Deep Sea Res., Part II*, *51*, 1435–1456.

Naveira Garabato, A. C., E. L. McDonagh, D. P. Stevens, K. J. Heywood, and R. J. Sanders (2002), On the export of Antarctic bottom water from the Weddell Sea, *Deep Sea Res., Part II*, *49*, 4715–4742.

Naveira Garabato, A. C., R. Ferrari, and K. L. Polzin (2011), Eddy stirring in the Southern Ocean, *J. Geophys. Res.*, *116*, C09019, doi:10.1029/2010JC006818.

Orsi, A. H., T. Whitworth, and W. D. Nowlin (1995), On the meridional extent and fronts of the Antarctic circumpolar current, *Deep Sea Res., Part I*, *42*, 641–673.

Owens, W. B., and N. G. Hogg, (1980), Oceanic observations of stratified Taylor columns near a bump, *Deep Sea Res., Part A*, *27*, 1029–1045.

Padman, L., H. A. Fricker, R. Coleman, S. Howard, and S. Erofeeva (2002), A new tidal model for the Antarctic ice shelves and seas, *Ann. Glaciol.*, *34*, 247–254.

Patara, L., and C. W. Böning (2014), Abyssal ocean warming around Antarctica strengthens the Atlantic overturning circulation, *Geophys. Res. Lett.*, *41*, 3972–3978, doi:10.1002/2014GL059923.

Patterson, S. L., and H. A. Sievers (1980), The Weddell-Scotia confluence, *J. Phys. Oceanogr.*, *10*, 1584–1610.

Perissinotto, R., and C. M. Duncombe-Rae (1990), Occurrence of anticyclonic eddies on the Prince Edward Plateau (Southern Ocean): Effects on phytoplankton biomass and production, *Deep Sea Res., Part A*, *37*, 777–793.

Proudman, J. (1916), On the motion of solids in a liquid posessing vorticity, *Proc. R. Soc. London*, *A92*, 408–424.

Smethie, W. M., P. Schlosser, G. Bönisch, and T. S. Hopkins (2000), Renewal and circulation of intermediate waters in the Canadian Basin observed on the SCICEX 96 cruise, *J. Geophys. Res.*, *105*, 1105–1121.

Taylor, G. I. (1923), Experiments on the motion of solid bodies in rotating fluids, *Proc. R. Soc. London*, *106*, 213–218.
Thompson, A. F., and M. K. Youngs (2013), Surface exchange between the Weddell and Scotia Seas, *Geophys. Res. Lett.*, *40*, 5920–5925, doi: 10.1002/2013GL058114.
Thompson, A. F., K. J. Heywood, S. E. Thorpe, A. H. H. Renner, and A. T. Castro (2009), Surface circulation at the tip of the Antarctic Peninsula from drifters, *J. Phys. Oceanogr.*, *39*, 3–26.
Tulloch, R., R. Ferrari, O. Jahn, A. Klocker, J. LaCasce, J. R. Ledwell, J. Marshall, M.-J. Messias, K. Speer, and A. Watson (2014), Direct estimate of lateral eddy diffusivity upstream of Drake passage, *J. Phys. Oceanogr. 44*, 2593–2616, doi:10.1175/JPO-D-13-0120.1 .
Whitworth, T., W. D. Nowlin, A. H. Orsi, R. A. Locarnini, and S. G. Smith (1994), Weddell sea shelf water in the Bransfield Strait and Weddell-Scotia confluence, *Deep Sea Res., Part I*, *41*, 629–641.
Yuan, X. (2004), ENSO-related impacts on Antarctic sea ice: Synthesis of phenomemon and mechanisms, *Antarct. Sci.*, *16*, 415–425.